Int J Clin Exp Pathol 2015;8(9):10228-10238
www.ijcep.com /ISSN:1936-2625/IJCEP0013614

Original Article

Changes of mesenchymal stromal cells mobilization and bone turnover in an experimental bone fracture model in ovariectomized mice

Jian Pang[1*], Hai-Ling Guo[1*], Dao-Fang Ding[1], Yu-Yun Wu[1], Yong-Fang Zhao[1], Xin-Feng Gu[2], Yu-Xin Zheng[2]

[1]Research Institute of Orthopedics, Shuguang Hospital Affiliated to Shanghai University of Traditional Chinese Medicine, Shanghai 201203, China; [2]Department of Orthopedics, Shuguang Hospital Affiliated to Shanghai University of Traditional Chinese Medicine, Shanghai 201203, China. [*]Equal contributors.

Received July 29, 2015; Accepted August 28, 2015; Epub September 1, 2015; Published September 15, 2015

Abstract: Objective: The aim of this study was to characterize the mesenchymal stromal cells (MSCs) and endothelial progenitor cells (EPCs) mobilization, and bone turnover in osteoporotic fracture healing in ovariectomized mice. Methods: In total, 112 female C57/BL mice were divided into two groups. The first group was sham-operated (SO), and the other group was ovariectomized (OVX). After three weeks, the right femora of the mice were fractured under anesthesia and internally fixed with steel pin. Peripheral blood and bone marrow were was collected for flow cytometry analysis, at 0 hours (h), 12 h, 24 h, 72 h and 168 h after fracture. MSCs and EPCs levels were assessed using cell surface antigens in different combinations (CD44+ CD34-CD45-, and CD34+ KDR+CD45-) by flow cytometry. At 0, 14, 28 and 42 days after fracture, sera were assayed for circulating levels of procollagen type I-N-terminal propeptide (P1NP) and C-terminal telopeptide of type I-collagen (CTX) by ELISA. Femurs were harvested at 2 weeks and 6 weeks after fracture for X-ray radiography, micro-computed tomography (micro-CT) and histology. Results: Our results showed that bone marrow and peripheral blood MSCs numbers of the OVX mice were significantly lower than the SO mice, at 12 h, 24 h and 72 h after fracture. In addition, circulating P1NP and CTX levels of the OVX mice were significantly higher than the SO mice, at 2 and 4 weeks. Conclusion: Results of the present study revealed disorders of bone marrow MSCs mobilization and bone turnover may partially account for the delay of osteoporotic fracture healing.

Keywords: Osteoporosis, bone healing, MSCs, mobilization, mouse

Introduction

Osteoporosis is a major health problem affecting elderly population. It is characterized by microarchitectural deterioration of bone structure, low bone mineral density, increased fragility and susceptibility to fracture [1]. Clinically, osteoporotic fractures are associated with an increased rate of implant failure and hampers functional recovery [2]. Furthermore, impaired fracture healing may result in significant morbidity and negatively impact quality of life [3]. Previous studies have also showed that osteoporosis impaired the fractures healing in animal models [4, 5]. Now much attention has been focused on fracture prevention, however, less focus has been given to osteoporotic fractures. Moreover, antiresorptive and anabolic drugs' effects on the fracture healing are subject to confirmation, although they could improve the outcome of osteoporosis. Therefore, osteoporotic fracture is still an unsolved problem to the surgeon as well as for the patient [6].

Bone fracture healing is a sophisticated process and the precise regulatory mechanisms of it are still not clearly understood [7]. It is known that fracture healing can occur by primary or secondary healing, which involve multiple biological responses, including mobilization and recruitment of stem and progenitor cells. Moreover, malfunctioning of bone marrow mesenchymal stromal cells (MSCs) is essential for osteoporosis [8]. Therefore, we inferred impaired bone fracture healing in osteoporotic

conditions may partly be due to disorder of bone marrow stem or progenitor cells. Next, an underlying mechanism in all cases of osteoporosis is an imbalance of bone resorption and formation, leading to disorder of bone remodeling. It is well known that the bone callus modeling and remodeling is also an important step of the process of bone fracture healing. Thus, the disorder of bone turnover/remodeling is also a possible mechanism of delay of osteoporotic fracture.

In this study, we wanted to observe the effect of ovariectomy-induced osteoporosis on fracture healing in a mouse model. Furthermore, we sought to characterize the MSCs and endothelial progenitor cells (EPCs) mobilization and bone turnover in osteoporotic fracture. We hypothesized that under ovariectomy-induced osteoporotic conditions, MSCs and/or EPCs levels are reduced due to impaired cells mobilization from the bone marrow in association with delay of the fracture healing.

Methods

Animals

One hundred and twelve 8-week-old female C57/BL mice (Sino-British Sippr/BK Lab Animal Ltd., Shanghai, China) weighing between 20 and 25 g were used. The mice were randomly divided into two groups: the first group (SO group) was sham-operated while the other group (OVX group) was ovariectomized. These mice were untreated for 3 weeks to allow the bones of the OVX mice to become osteoporotic [9]. To verify the success of OVX, estrogen levels (pg/mL) were measured from blood samples collected at 3 weeks after ovariectomy operation. Serum estrogen measurements were performed by the existing systems (Roche/Hitachi Modular Analytics Hybrid; Roche Diagnostics, Mannheim, Germany).

All animals received a standard laboratory diet (containing 1.56% calcium, 0.8% phosphorus and 800 IU/kg vitamin D), water ad libitum and accommodated in cages of a centralized animal house with 12 h day-night light condition, 60% humidity and room temperature of 21°C. Every eight animals were kept in one cage. The experimental protocols for animal care and experiment management were approved by the Scientific and Ethics Committees at the Shanghai University of Traditional Chinese Medicine. Animals were cared for according to the Chinese national regulations for experimental animal care and study.

Fractured method

The right femurs of all mice were fractured aseptically according to protocol described by Diwan et al. [10], at 3 weeks after ovariectomy. A controlled mid-shaft femoral fracture was made by dental electric micro motor unit (Strong 102, Saeshin, KR) with a circular saw. The thickness of the saw was 0.15 mm. The fracture was then fixed with a 0.45-mm-diameter stainless steel pin, which was passed retrograde into the proximal fragment and then into the medullary canal of the distal fragment.

At 0 hours (h), 12 h, 24 h, 72 h and 168 h after fracture, the equal number (n = 8) of mice in every group was sacrificed, and MSCs and EPCs in peripheral blood and bone marrow were quantified. At 2 weeks and 6 weeks, the equal number of mice was sacrificed; the right femurs were harvested, and fixed immediately in 10% neutral buffered formalin for radiological and histological study.

Flow cytometric analysis

MSCs and EPCs in peripheral blood and bone marrow were quantified at 0 h, 12 h, 24 h, 72 h and 168 h after fracture. Peripheral blood 500-1000 μL was collected from anesthetized mice by means of cardiac puncture into 100 μL of 10 mmol/L ethylenediamine tetra-acetic acid (EDTA) in phosphate buffered saline to prevent coagulation. Bone marrow was collected immediately after death by isolation of the left femur and removal of all soft tissue and all articular surfaces except that of the proximal femur. Femurs were then crushed with a mortar and pestle in a solution of 10 mmol/L EDTA in phosphate buffered saline, and supernatant from the bone wash was collected, filtered through 70-μm nylon mesh and further process as described below.

MSCs and EPCs levels were assessed by flow cytometry using cell surface antigens in different combinations (CD44+ CD34-CD45-, and CD34+ KDR+CD45-) as previously reported [11, 12]. Briefly, before staining with specific monoclonal antibodies, samples were washed

with phosphate buffered saline. Next, 100 μL of peripheral blood or bone marrow sample was incubated with 10 μL of FITC- conjugated CD34 monoclonal antibody (mAb) (BD Biosciences, San Jose, CA), 5 μL of PE-conjugated CD44 mAb (BD Biosciences, San Jose, CA), and 5 μL of PC5-conjugated CD45 mAb (BD Biosciences, San Jose, CA). The another 100 μL of peripheral blood or bone marrow sample was incubated with 10 μL of FITC- conjugated CD34 mAb (BD Biosciences, San Jose, CA), 5 μL of PE-conjugated KDR mAb (R&D Systems, Minneapolis, MN), and 5 μL of PC5-conjugated CD45 mAb (BD Biosciences, San Jose, CA). All samples were incubated at 4°C for 30 minutes. The samples were lysed before flow cytometry analysis. Cell suspensions were evaluated by flow cytometry (Beckman Coulter, Miami, Florida, USA). The numbers of EPCs and MSCs were determined by a two-dimensional side-scatter fluorescence dot-plot analysis of the sample after gating on the lymphocyte population.

X-ray radiography

X-rays were performed on the right fractured femurs in the mediolateral planes using a high-resolution digital radiography system (model MX-20; Faxitron X-Ray, Wheeling, IL). X-ray digitized radiographs of the femurs were taken with exposure time of 1.5 s at tube voltage 28 kVp. Fracture healing was staged on the X-ray radiographs using a radiographic scoring system according to protocol described by Shuid et al. [13]. The callus staging was also assessed using a scoring system according to protocol described by Shuid et al. [14]. Two experienced researcher, who were blinded to the grouping and time points of the study, performed independent assessments of the bone fracture healing status and callous status on digitized radiographs.

Micro-computed tomography (micro-CT) measurement

Before micro-CT scanning, the stainless steel pins were extracted. These specimens were scanned on a desktop micro-CT system (Explore Locus SP; GE Healthcare, London, Ontario, Canada) for a detailed qualitative and quantitative three-dimensional (3-D) evaluation. The scanning system was set to 80 kV, 80 μA, and 2960-milliseconds exposure time, with an isotropic voxel size of 12 μm. Bone density was normalized using an acrylic calibration phantom that included densities equivalent to air, water and bone.

Image reconstruction and analysis was performed by Microview with ABA (Version 2.3; GE Healthcare, London, Ontario, Canada). A 5-mm-long polygonal region of interest (ROI) centered at the fracture plane according to protocol of Warden et al. [15], and cortical bone was eliminated. Mineralized tissue was segmented from air or soft tissue at threshold of 1758 HU (corresponding to BMD = 300 mg HA/cm^3). Calculated parameters included callus volume, fraction of mineralized callus (BV/TV), bone mineral density (BMD, average attenuation value of bone and non-bone tissue) and tissue mineral density (TMD, average attenuation value of bone tissue only).

Enzyme-linked immunosorbent assay (ELISA)

At 0, 14, 28 and 42 days after fracture, sera were collected from vein in the eye pit. Sera were assayed for circulating levels of procollagen type I-N-terminal propeptide (P1NP) and C-terminal telopeptide of type I-collagen (CTX) by ELISA kit (Shanghai Xitang Biological Technology, Inc., China) following the manufacturer's protocol. Briefly, 50 μl serum was added to a polyclonal rabbit anti-P1NP or anti-CTX coated plate in duplicate and incubated with 50 μl biotinlabeled P1NP or CTX for 1 h and then 150 μl avidin-linked horseradish peroxidase was added to each well and incubated for 30 min. Finally, 150 μl tetramethylbenzidine substrate was added for color development, which was measured using a multi-mode microplate reader (BioTek Synergy, BioTek Instruments, Inc., VT, USA) within 30 min of adding stop solution. Standard curves were generated using serial dilutions of the P1NP or CTX calibration standards supplied in the ELISA kit. The expression levels were normalized to baseline (day 0 serum).

Histology

The specimens were fixed in 10% neutral buffered formalin, and then decalcified with 0.5 M ethylenediaminetetraacetic acid (pH 7.4) at 37°C for 15 days. Afterwards, dehydration with a series of ethanol rinses and that of xylene, the specimens were embedded in paraffin wax. A 5-μm thick sections were cut along the longi-

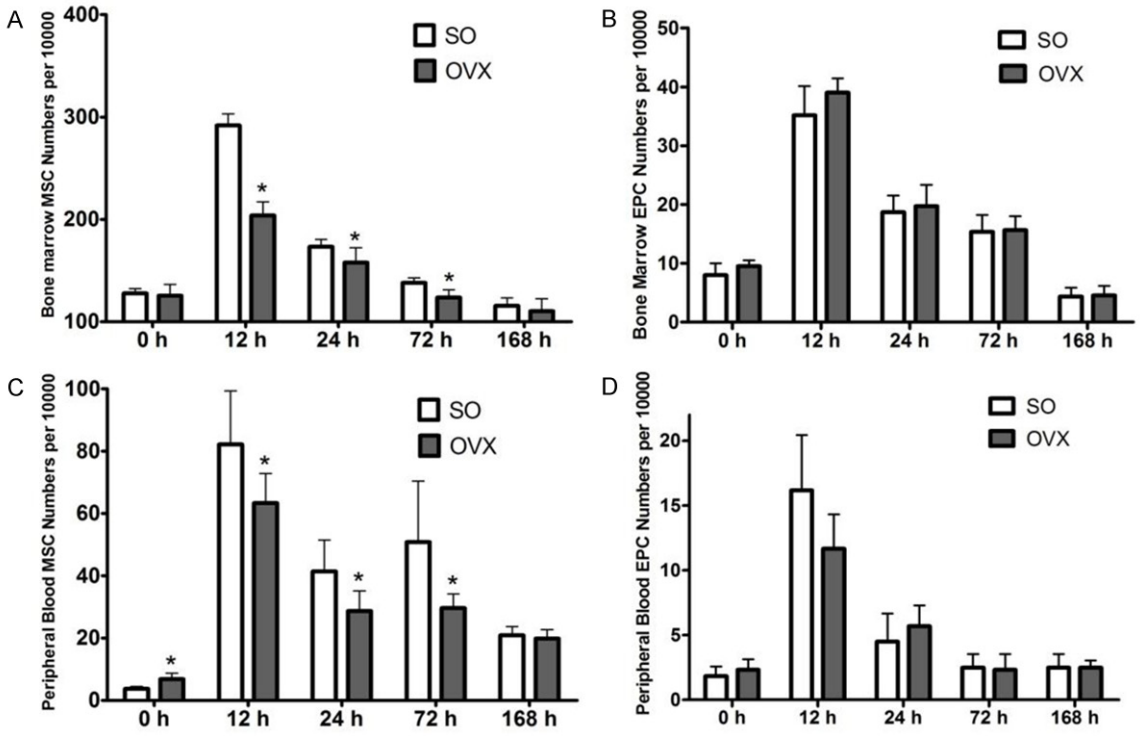

Figure 1. A-D: MSCs and EPCs in peripheral blood and bone marrow were quantified at 0 h, 12 h, 24 h, 72 h and 168 h post-fracture, and statistically analyzing. Error bars represent SD. *Significant difference compared to SO group; $P < 0.05$.

tudinal axis of femur by a rotary microtome (Leica RM2165, Leica, Germany) and mounted on glass slides, then stained with Safarin-O/Fast green method to allow identification of bone and cartilage and evaluated qualitatively under light microscopy (Olympus BX43F with Olympus U-CBS digital camera, Olympus, Japan).

Statistical analyses

Data were expressed as mean ± standard deviation (SD). All statistical comparisons were done with SPSS 19.0 (SPSS Inc., Chicago, IL, USA) for Windows software. For normally distributed data, the statistical test used was *t-test*. Data that were not normally distributed were analyzed using *Mann–Whitney test*. Differences between means at the 5% confidence level ($P < 0.05$) were considered statistically significant.

Results

All the mice recovered well after the ovariectomy and fracture operation, and did not display any signs of infection. No statistically significant differences in baseline values and changes of body weight between two groups were found. At 3 weeks post-ovariectomy, no estrogen (< 1 ng/mL) could be detected in OVX mice, estrogen could be detected in SO mice (25.72±9.06 ng/mL).

Flow cytometric analysis

MSCs and EPCs in bone marrow and peripheral blood were identified from mononuclear cell by the fluorescent antibodies. Bone marrow MSCs numbers significantly increased after fracture, and then decreased from 12 h post-fracture. At 12 h, 24 h and 72 h post-fracture, bone marrow MSCs numbers of the OVX group were significantly lower than the SO group ($P < 0.05$). There was no significant difference between the two groups at 168 h. (**Figure 1A**) Peripheral blood MSCs numbers also significantly increased after fracture, and reached the highest level on 12 h post-fracture. At 12 h, 24 h and 72 h post-fracture, peripheral blood MSCs numbers of the OVX group were significantly lower than the SO group ($P < 0.05$). There was no significant difference between the two groups at 168 h (**Figure 1C**).

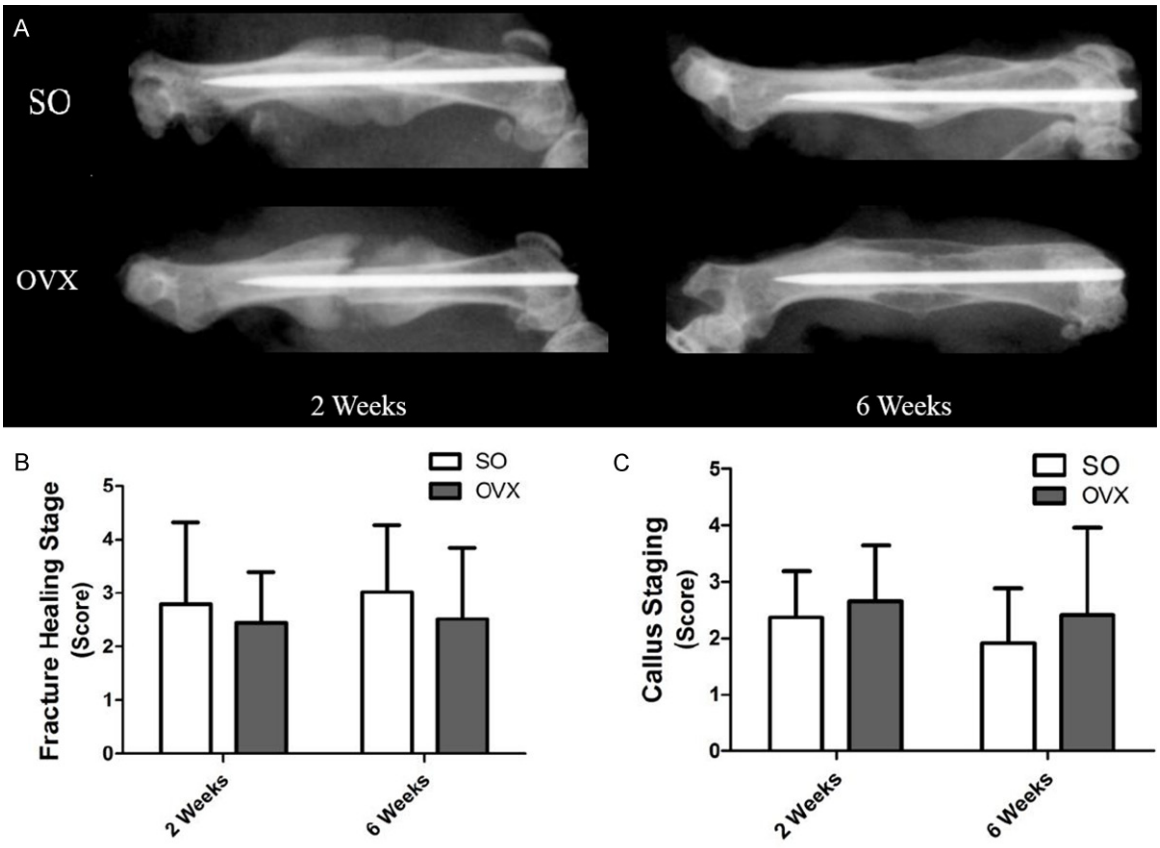

Figure 2. A: Representative X-ray radiographs 2 weeks and 6 weeks post-fracture for the SO and the OVX groups. B and C: Radiological assessments on fracture healing by callus staging and fracture healing stage score of the X-ray images, and statistically analyzing. Error bars represent SD. *Significant difference compared to SO group; $P < 0.05$.

EPCs numbers in bone marrow and peripheral blood also significantly increased after fracture, and reached the highest level on 12 h post-fracture. But, there was no significant difference between the two groups at both time point (**Figure 1B** and **1D**).

X-ray radiography

Representative X-ray digitized radiographs of the femurs are showed as **Figure 3A**. At 2 weeks post-fracture (**Figure 2B**, **2C**), no statistically different scores of fracture healing stage and callus was found between the two groups. At 6 weeks (**Figure 2B**, **2C**), there were also not statistically different scores of fracture healing stage and callus. However, the OVX group had lower trending scores in fracture healing stage and higher trending scores in callus staging, compared to the SO group.

Micro-computed tomography

Representative 3D-reconstructed micro-CT images are showed as **Figure 3A**. At 2 weeks post-fracture (**Figure 3B-E**), no statistically significant differences in callus volume, BV/TV, BMD and TMD between the two groups, OVX animals' mean values trended higher in volume, BMD and TMD, lower in BV/TV, than SO. At 6 weeks (**Figure 3B-E**), the OVX group had significantly lower BV/TV and BMD values than the control ($P < 0.05$), and no significant differences in volume and TMD were observed between the groups.

Enzyme-linked immunosorbent assay

Biomarkers of bone turnover, including P1NP (bone formation marker) and CTX (bone resorption marker), provide a means of evaluating skeletal dynamics. Circulating P1NP levels significantly increased after fracture, and then decreased from 2 weeks post-fracture. At 2 and 4 weeks post-fracture, circulating P1NP levels of the OVX group were significantly higher than the SO group ($P < 0.05$). There was no significant difference between the two groups at 6 weeks (**Figure 4A**).

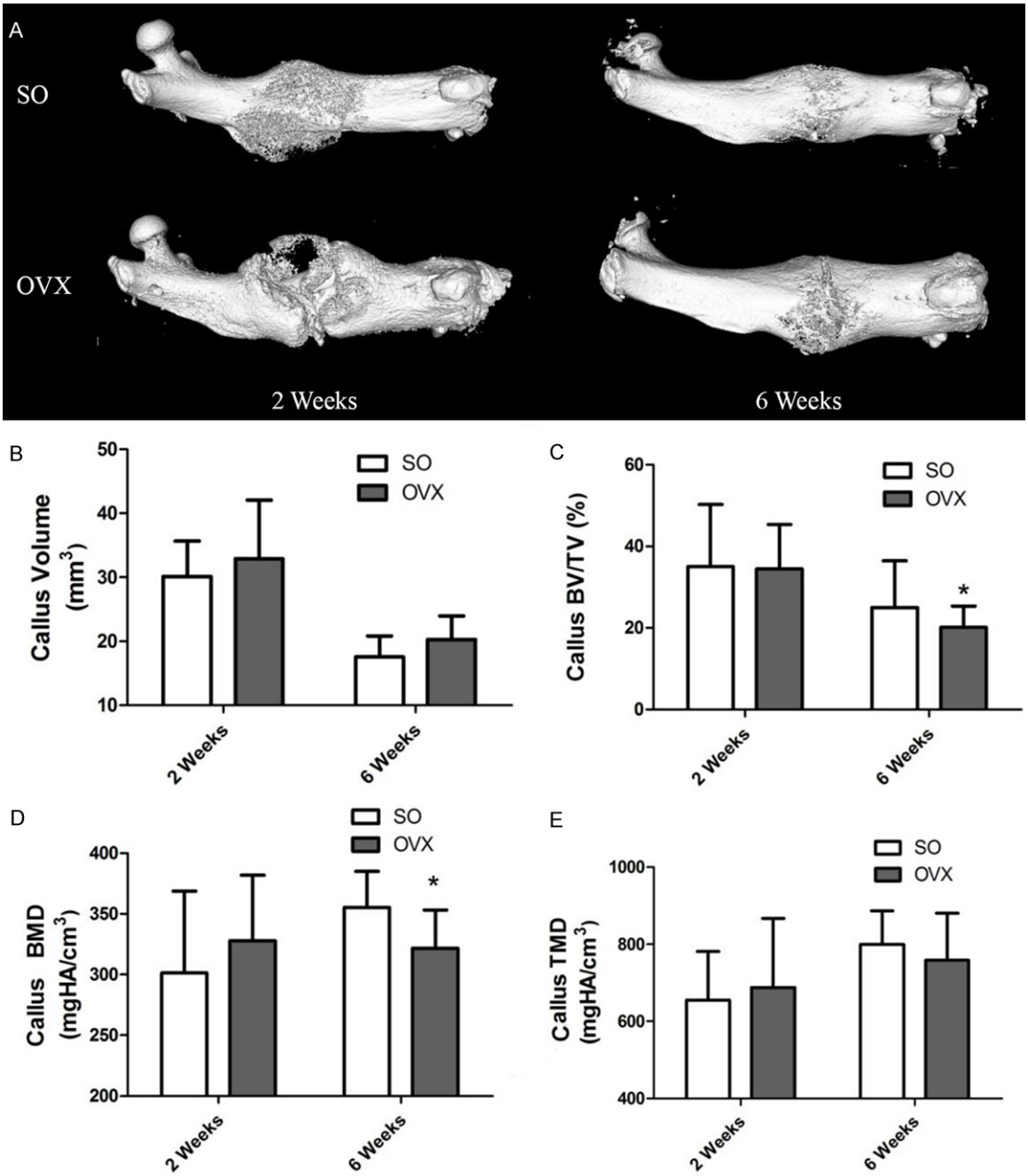

Figure 3. A: Representative micro-CT images of fractured femora. B-E: Micro-CT assessments on fracture healing by measuring the callus volume, BV/TV, BMD and TMD, and statistically analyzing. Error bars represent SD. *Significant difference compared to SO group; $P < 0.05$.

Circulating CTX levels also significantly increased after fracture, and then decreased from 2 weeks post-fracture. At 2 and 4 weeks post-fracture, circulating CTX levels of the OVX group were also significantly higher than the SO group ($P < 0.05$). There was no significant difference between the two groups at 6 weeks (**Figure 4B**).

Histology

Representative histological images are showed in **Figure 5**. At 2 weeks post-fracture, abundant amounts of chondroid and osseous tissue were found beneath periosteum adjacent to the fracture gaps in both groups. In OVX group, significant fracture end resorption was observed.

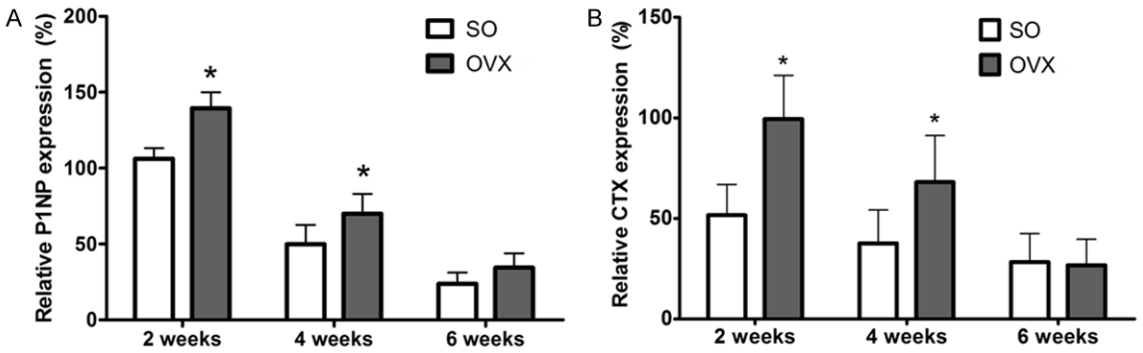

Figure 4. A, B: Circulating P1NP and CTX levels were tested by ELISA at 0, 14, 28 and 42 days post-fracture. The expression levels were normalized to baseline (day 0). Error bars represent SD. *Significant difference compared to SO group; $P < 0.05$.

Additionally, more chondrocytes was found in the fracture callus taken from the OVX group. At 6 weeks, osseous tissue had replaced chondroid tissue. Hard callus remodeling was going on with more mature and tightly arranged woven or lamellar bone across the fracture gap in the SO group compared to the OVX group.

Discussion

The present study showed that fracture healing was impaired in osteoporotic fracture in an ovariectomized mouse model, based on radiological and histological assessment. Notably, the results of this study revealed disorders of bone marrow MSCs mobilization and bone turnover in osteoporotic fracture.

The results of this study supported that fracture healing is impaired in osteoporotic condition. The OVX significantly lowered callus BV/TV and BMD at 6 weeks. Histological images of the healing fractures in the OVX mice found hastening of broken end resorption and delay of hard callus remodeling. Moreover, bone marrow and peripheral blood MSCs numbers of the OVX mice were significantly lower than the SO mice, at 12 h, 24 h and 72 h after fracture. In addition, circulating P1NP and CTX levels of the OVX mice were significantly higher than the SO mice, at 2 and 4 weeks post-fracture. These suggested that impaired mobilization of bone marrow MSCs and imbalance of bone turnover were potential mechanisms of delay of osteoporotic fracture.

Although evidence is inconclusive, some studies suggested that bone fracture healing is delayed in the presence of osteoporosis in humans [4, 16, 17]. Many previous studies using animal models have also confirmed that ovariectomy-induced osteoporosis impairs fracture healing at different stages [4, 5, 18-22]. The results of callus BMD in our study was consistent with previous reports [20, 23]. Additionally, delay of hard callus remodeling as showed by micro-CT and histological images, both suggested the delay of fracture healing in the OVX animals. The impairment of osteoporotic fracture healing may be resulted from multiple factors. These factors include impaired angiogenesis, decrease in growth hormone secretion, and poor sensitivity of osteoblasts to mechanical signals [24-26]. Additionally, a recent study reported that the delayed healing rate and impaired callus quality in ovariectomy-induced osteoporotic fracture is related to the delayed expression of ERs. A high ER-α: ER-β ratio favors callus formation [27]. But, as for the precise regulation mechanisms of osteoporotic fracture healing, they are still not fully understood.

We demonstrated the mobilization of bone marrow MSCs was impaired in osteoporotic fracture. However, there was no the same event observed in EPCs. Bone marrow contains a variety of stem and progenitor cells that participate in bone healing, including MSCs and EPCs [28, 29]. Generation of stem and progenitor cells from the bone marrow is a major response to tissue repair. Each of these cell types has been independently proposed to support bone healing [30, 31]. MSCs give rise to chondroblasts and osteoblasts for tissue repair [32];

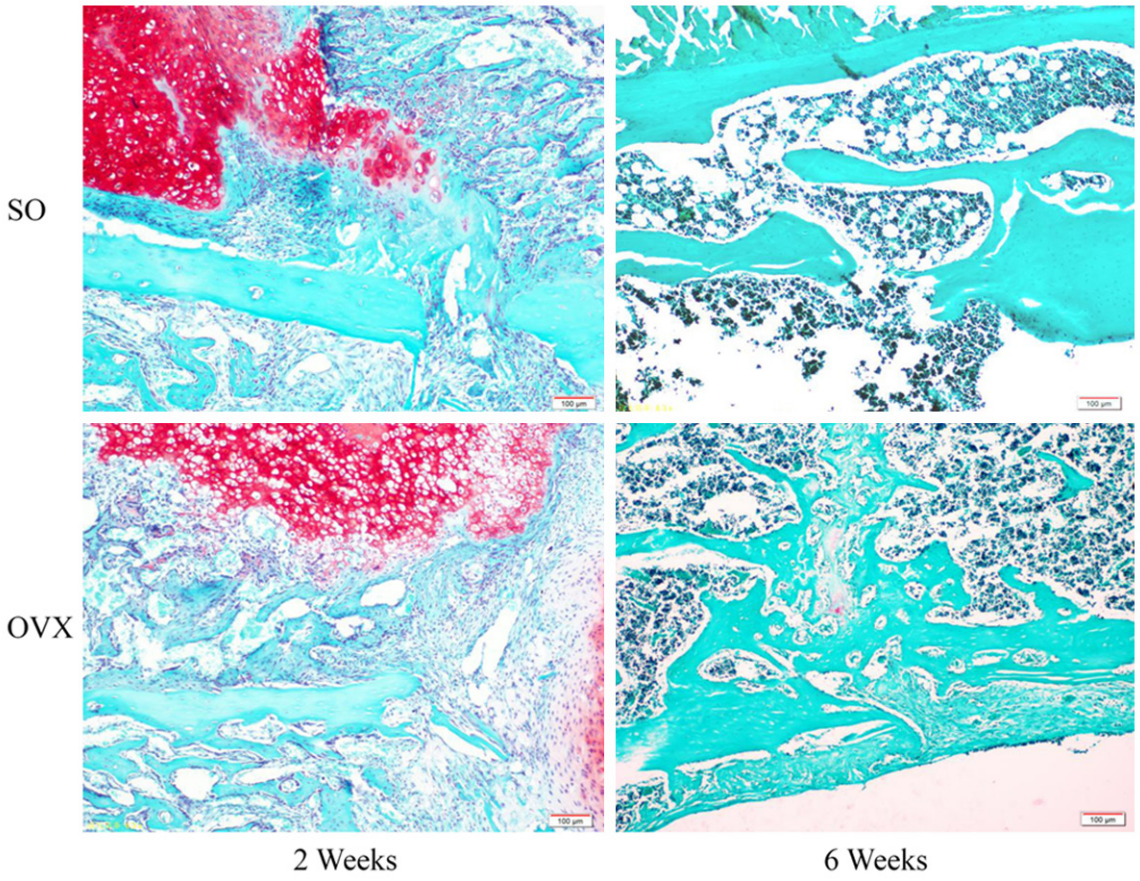

Figure 5. Representative histological images 2 and 6 weeks post-fracture for the SO and the OVX groups. Sections were stained using the Safarin-O/Fast green method which stains bone and cartilage blue/green and red, respectively. Scale bar represents 100 μm.

EPCs revascularize the injury site and provide access for other types of stem cells to populate the callus [33]. Under normal physiological conditions, there are few circulating MSCs and EPCs in peripheral blood [34, 35]. Emerging evidence suggested that MSCs can potentially be mobilized into the circulation in response to injury signals and exert their reparative effects at the site of injury. Several studies have reported that the number of MSCs detected in circulation was markedly increased after tissue damage such as acute burn, muscle injury and cardiopulmonary injury. MSCs can also egress into the peripheral blood during fracture and osteoporosis. Although the role of circulating MSCs in bone healing remains controversial, a recent study formally demonstrated the participation of circulating MSCs in a mouse model of fracture healing [36]. As the progenitor of osteoblasts, MSCs were capable of migrating from their location into the circulation probably on their way to the impaired bone [37]. EPCs numbers in peripheral blood are significantly increased in association with vascular injury, burns and bone fracture [33]. We found the MSCs and EPCs numbers in bone marrow and peripheral blood significantly increased after fracture as previous reports. Furthermore, the bone marrow and peripheral blood MSCs numbers of the OVX mice were significantly lower than the SO mice.

Biomarkers of bone turnover have long been used to complement the radiological assessment of patients with bone disease. They reflect the metabolic activity of the entire skeleton. Quantitative changes in bone turnover can be assessed easily and non-invasively by the measurement of bone turnover biomarkers [38]. Osteoporosis of the elderly referred to as senile osteoporosis is due to impairment of bone formation. However, the main reason of post-

menopausal osteoporosis is high bone turnover due to increased osteoclastic activity. It is known that estrogen deficiency is a major contributory factor to postmenopausal osteoporosis. Estrogen inhibits the activation of bone remodeling, via the osteocytes, and also inhibits bone resorption, largely by direct actions on osteoclasts [39]. Biomarkers of bone turnover, including P1NP (bone formation marker) and CTX (bone resorption marker), provided a means of evaluating skeletal dynamics [40]. Our study showed circulating P1NP and CTX levels significantly increased after fracture, and then decreased from 2 weeks post-fracture. At 2 and 4 weeks post-fracture, circulating P1NP and CTX levels of the OVX group were significantly higher than the SO group. This revealed the impairment of bone turnover may be a mechanism of delay of osteoporotic fracture.

Our study also has a few limitations. Firstly, the fracture bones were not evaluated with biomechanical testing. Although biomechanical testing has been used extensively in fracture studies and is widely considered the gold standard of fracture repair assessment. However, applying such tests to mouse fracture models might result in significant variability [41]. Thus assessments based on micro-CT were considered to be more practical for evaluating the healing femur in the mouse fracture model [42]. In addition, advanced methods such as finite element analysis (FEA) or structural rigidity analysis can utilize micro-CT scans to predict failure strength [43]. Secondly, our study only analyzed outcomes of fracture healing at two time point and future experiments should study whether osteoporosis might confer changes in the dynamics of fracture healing by investigating other time points. Additionally, the molecular mechanisms responsible for MSCs mobilization and bone remodeling in osteoporotic fracture have not yet been investigated. The characterizations of MSCs migration to the fracture site during fracture repair still remain to be observed also.

Conclusion

In summary, results of the present study demonstrated that fracture healing was impaired in a mouse model of osteoporotic fracture once again. Notably, the results suggested that the impairments of mobilization of bone marrow MSCs and bone turnover were potential mechanisms of delay of osteoporotic fracture. Further investigations are required.

Acknowledgements

This work was supported by the National Natural Science Foundation of China (Grant no. 81102603, 81173277, 81173621, 81403415). None of the authors have a conflict of interest to report.

Disclosure of conflict of interest

None.

Address correspondence to: Dr. Jian Pang, Research Institute of Orthopedics, Shuguang Hospital Affiliated to Shanghai University of Traditional Chinese Medicine, Shanghai 201203, China. Tel: +86 21 20256519; E-mail: pangjian2004@gmail.com; Dr. Yu-Xin Zheng, Department of Orthopedics, Shuguang Hospital Affiliated to Shanghai University of Traditional Chinese Medicine, Shanghai 201203, China. E-mail: ZhengYuXin2000@126.com

References

[1] Pop A, Huttenhower C, Iyer-Pascuzzi A, Benfey PN, Troyanskaya OG. Integrated functional networks of process, tissue, and developmental stage specific interactions in Arabidopsis thaliana. BMC Syst Biol 2010; 4: 180.

[2] Giannoudis PV, Schneider E. Principles of fixation of osteoporotic fractures. J Bone Joint Surg Br 2006; 88: 1272-1278.

[3] Ensrud KE, Thompson DE, Cauley JA, Nevitt MC, Kado DM, Hochberg MC, Santora AC 2nd, Black DM. Prevalent vertebral deformities predict mortality and hospitalization in older women with low bone mass. Fracture Intervention Trial Research Group. J Am Geriatr Soc 2000; 48: 241-249.

[4] Giannoudis P, Tzioupis C, Almalki T, Buckley R. Fracture healing in osteoporotic fractures: is it really different? A basic science perspective. Injury 2007; 38 Suppl 1: S90-99.

[5] Egermann M, Goldhahn J, Schneider E. Animal models for fracture treatment in osteoporosis. Osteoporos Int 2005; 16 Suppl 2: S129-138.

[6] Abd Jalil MA, Shuid AN, Muhammad N. Role of medicinal plants and natural products on osteoporotic fracture healing. Evid Based Complement Alternat Med 2012; 2012: 714512.

[7] Einhorn TA. The cell and molecular biology of fracture healing. Clin Orthop Relat Res 1998; Suppl: S7-21.

[8] Pino AM, Rosen CJ, Rodriguez JP. In osteoporosis, differentiation of mesenchymal stem cells

(MSCs) improves bone marrow adipogenesis. Biol Res 2012; 45: 279-287.
[9] Binder NB, Niederreiter B, Hoffmann O, Stange R, Pap T, Stulnig TM, Mack M, Erben RG, Smolen JS, Redlich K. Estrogen-dependent and C-C chemokine receptor-2-dependent pathways determine osteoclast behavior in osteoporosis. Nat Med 2009; 15: 417-424.
[10] Diwan AD, Wang MX, Jang D, Zhu W, Murrell GA. Nitric oxide modulates fracture healing. J Bone Miner Res 2000; 15: 342-351.
[11] Weidenhielm L, Svensson OK, Brostrom Lk. Surgical correction of leg alignment in unilateral knee osteoarthrosis reduces the load on the hip and knee joint bilaterally. Clin Biomech (Bristol, Avon) 1995; 10: 217-221.
[12] Ranu HS. An evaluation of the centre of pressure for successive steps with miniature triaxial load cells. J Med Eng Technol 1998; 12: 164-166.
[13] Shuid AN, Mohamad S, Muhammad N, Fadzilah FM, Mokhtar SA, Mohamed N, Soelaiman IN. Effects of alpha-tocopherol on the early phase of osteoporotic fracture healing. J Orthop Res 2011; 29: 1732-1738.
[14] Shuid AN, Mohamad S, Mohamed N, Fadzilah FM, Mokhtar SA, Abdullah S, Othman F, Suhaimi F, Muhammad N, Soelaiman IN. Effects of calcium supplements on fracture healing in a rat osteoporotic model. J Orthop Res 2010; 28: 1651-1656.
[15] Warden SJ, Komatsu DE, Rydberg J, Bond JL, Hassett SM. Recombinant human parathyroid hormone (PTH 1-34) and low-intensity pulsed ultrasound have contrasting additive effects during fracture healing. Bone 2009; 44: 485-494.
[16] Madsen JL. Bone SPECT/CT detection of a sequestrum in chronic-infected nonunion of the tibia. Clin Nucl Med 2008; 33: 700-701.
[17] Zhang CQ, Cheng XG, Sheng JG, Li HS, Su Y, Xu J, Zeng BF. [The surgical technique and follow-up of the treatment with locking internal fixation on long bone nonunion of extremities]. Zhonghua Wai Ke Za Zhi 2008; 46: 510-513.
[18] Wang JW, Li W, Xu SW, Yang DS, Wang Y, Lin M, Zhao GF. Osteoporosis influences the middle and late periods of fracture healing in a rat osteoporotic model. Chin J Traumatol 2005; 8: 111-116.
[19] Namkung-Matthai H, Appleyard R, Jansen J, Hao Lin J, Maastricht S, Swain M, Mason RS, Murrell GA, Diwan AD, Diamond T. Osteoporosis influences the early period of fracture healing in a rat osteoporotic model. Bone 2001; 28: 80-86.
[20] Hao YJ, Zhang G, Wang YS, Qin L, Hung WY, Leung K, Pei FX. Changes of microstructure and mineralized tissue in the middle and late phase of osteoporotic fracture healing in rats. Bone 2007; 41: 631-638.
[21] Shi HF, Cheung WH, Qin L, Leung AH, Leung KS. Low-magnitude high-frequency vibration treatment augments fracture healing in ovariectomy-induced osteoporotic bone. Bone 2010; 46: 1299-1305.
[22] Mohamad S, Shuid AN, Mohamed N, Fadzilah FM, Mokhtar SA, Abdullah S, Othman F, Suhaimi F, Muhammad N, Soelaiman IN. The effects of alpha-tocopherol supplementation on fracture healing in a postmenopausal osteoporotic rat model. Clinics (Sao Paulo) 2012; 67: 1077-1085.
[23] Ding WG, Zhang ZM, Zhang YH, Jiang SD, Jiang LS, Dai LY. Changes of substance P during fracture healing in ovariectomized mice. Regul Pept 2010; 159: 28-34.
[24] Cheung WH, Chow SK, Sun MH, Qin L, Leung KS. Low-intensity pulsed ultrasound accelerated callus formation, angiogenesis and callus remodeling in osteoporotic fracture healing. Ultrasound Med Biol 2011; 37: 231-238.
[25] Zhang G, Qin L, Hung WY, Shi YY, Leung PC, Yeung HY, Leung KS. Flavonoids derived from herbal Epimedium Brevicornum Maxim prevent OVX-induced osteoporosis in rats independent of its enhancement in intestinal calcium absorption. Bone 2006; 38: 818-825.
[26] Neidlinger-Wilke C, Stalla I, Claes L, Brand R, Hoellen I, Rübenacker S, Arand M, Kinzl L. Human osteoblasts from younger normal and osteoporotic donors show differences in proliferation and TGF beta-release in response to cyclic strain. J Biomech 1995; 28: 1411-1418.
[27] Chow SK, Leung KS, Qin L, Wei F, Cheung WH. Callus formation is related to the expression ratios of estrogen receptors-alpha and -beta in ovariectomy-induced osteoporotic fracture healing. Arch Orthop Trauma Surg 2014; 134: 1405-1416.
[28] Yu CP, Tsai SY, Kao LJ, Chao PD, Hou YC. A Chinese herb formula decreases the monocarboxylate transporter-mediated absorption of valproic acid in rats. Phytomedicine 2013; 20: 648-653.
[29] Jia P, Chen G, Zhou G, Zhong Y, Li R. Fuyuan Decoction inhibits nitric oxide production via inactivation of nuclear factor-kappaB in SW1353 chondrosarcoma cells. J Ethnopharmacol 2013; 146: 853-858.
[30] Gao R, Lin Y, Liang G, Yu B, Gao Y. Comparative pharmacokinetic study of chlorogenic acid after oral administration of Lonicerae Japonicae Flos and Shuang-Huang-Lian in normal and febrile rats. Phytother Res 2014; 28: 144-147.
[31] Huang J, Tao J, Xue X, Yang S, Han P, Lin Z, Xu W, Lin J, Peng J, Chen L. Gua Lou Gui Zhi decoction exerts neuroprotective effects on post-

stroke spasticity via the modulation of glutamate levels and AMPA receptor expression. Int J Mol Med 2013; 31: 841-848.
[32] Chen Y, Gao C, Ma Y, Qiu F. Pharmacokinetic study of multiple active constituents after oral gavage of Guizhi decoction in rats using a LC-MS/MS method. Eur J Drug Metab Pharmacokinet 2013; 38: 283-293.
[33] Wang X, Zhang A, Wang P, Sun H, Wu G, Sun W, Lv H, Jiao G, Xu H, Yuan Y, Liu L, Zou D, Wu Z, Han Y, Yan G, Dong W, Wu F, Dong T, Yu Y, Zhang S, Wu X, Tong X, Meng X. Metabolomics coupled with proteomics advancing drug discovery toward more agile development of targeted combination therapies. Mol Cell Proteomics 2013; 12: 1226-1238.
[34] Wong KC, Pang WY, Wang XL, Mok SK, Lai WP, Chow HK, Leung PC, Yao XS, Wong MS. Drynaria fortunei-derived total flavonoid fraction and isolated compounds exert oestrogen-like protective effects in bone. Br J Nutr 2013; 110: 475-485.
[35] Han W, Xiong Y, Li Y, Fang W, Ma Y, Liu L, Li F, Zhu X. Anti-arthritic effects of clematichinenoside (AR-6) on PI3K/Akt signaling pathway and TNF-alpha associated with collagen-induced arthritis. Pharm Biol 2013; 51: 13-22.
[36] Kitaori T, Ito H, Schwarz EM, Tsutsumi R, Yoshitomi H, Oishi S, Nakano M, Fujii N, Nagasawa T, Nakamura T. Stromal cell-derived factor 1/CXCR4 signaling is critical for the recruitment of mesenchymal stem cells to the fracture site during skeletal repair in a mouse model. Arthritis Rheum 2009; 60: 813-823.
[37] Wang Y, Wang XX, Zhang LN, Jin SM, Zhang J. Effects of traditional Chinese medicine on bone remodeling during orthodontic tooth movement. J Ethnopharmacol 2012; 141: 642-646.
[38] Li S, Lee K, Zhao J, Yang Z, He S, Weng X. Neural competition as a developmental process: early hemispheric specialization for word processing delays specialization for face processing. Neuropsychologia 2013; 51: 950-959.
[39] Faienza MF, Ventura A, Marzano F, Cavallo L. Postmenopausal osteoporosis: the role of immune system cells. Clin Dev Immunol 2013; 2013: 575936.
[40] Lippincott-Schwartz J. Bridging structure and process in developmental biology through new imaging technologies. Dev Cell 2011; 21: 5-10.
[41] Manigrasso MB, O'Connor JP. Characterization of a closed femur fracture model in mice. J Orthop Trauma 2004; 18: 687-695.
[42] O'Neill KR, Stutz CM, Mignemi NA, Burns MC, Murry MR, Nyman JS, Schoenecker JG. Micro-computed tomography assessment of the progression of fracture healing in mice. Bone 2012; 50: 1357-1367.
[43] Ranu HS. Normal and pathological human gait analysis using miniature triaxial shoe-borne load cells. Am J Phys Med 1987; 66: 1-11.